9318 *Biochemistry* **2010,** *49,* 9318–9327
DOI: 10.1021/bi101141d

BIOCHEMISTRY
including biophysical chemistry & molecular biology
*Article*

# Phosphatidylinositol 4,5-Bisphosphate-Induced Conformational Change of Ezrin and Formation of Ezrin Oligomers[†]

Kevin Carvalho,[‡,§] Nada Khalifat,[‡,#] Ofelia Maniti,[#,⊥] Claire Nicolas,[§,⊥] Stefan Arold,[∥,@] Catherine Picart,*[,§,⊥] and Laurence Ramos*[,‡]

[‡]*Laboratoire des Colloïdes, Verres et Nanomatériaux, UMR CNRS-UM2 n°5587, cc26, Université Montpellier 2, Place E. Bataillon, F-34095 Montpellier Cedex 5, France,* [§]*Dynamique des Interactions Membranaires Normales et Pathologiques, Université de Montpellier 2 et 1, CNRS, Place Eugène Bataillon, F-34095 Montpellier Cedex 5, France,* [∥]*Centre de Biochimie Structurale, Montpellier, France, and CNRS UMR 5048, INSERM U554, Université Montpellier I et II, F-34090 Montpellier, France,* [⊥]*Minatec, Grenoble Institute of Technology and LMGP, 3 parvis Louis Néel, F-38016 Grenoble Cedex, France, and* [@]*University of Texas M. D. Anderson Cancer Center, 1515 Holcombe Boulevard, Houston, Texas 77030, United States*
[#]*These authors contributed equally to this work.*

*Received March 2, 2010; Revised Manuscript Received September 7, 2010*

ABSTRACT: The plasma membrane−cytoskeleton interface is a dynamic structure involved in a variety of cellular events. Ezrin, a protein from the ERM family, provides a direct linkage between the cytoskeleton and the membrane via its interaction with phosphatidylinositol 4,5-bisphosphate ($PIP_2$). In this paper, we investigate the interaction between $PIP_2$ and ezrin in vitro using $PIP_2$ dispersed in a unimolecular way in buffer. We compared the results obtained with full-length ezrin to those obtained with an ezrin mutant, which was previously found not to be localized at the cell membrane, and with the N-terminal membrane binding domain (FERM domain) of ezrin. We show that $PIP_2$ induced a conformational change in full-length ezrin. $PIP_2$ was also found to induce, in vitro, the formation of oligomers of wild-type ezrin, but not of mutant ezrin. These oligomers had previously been observed in vivo, but their role is yet to be clarified. Our finding hints at a possible role for $PIP_2$ in the formation of ezrin oligomers.

Phosphoinositides make up a particular class of lipids present in cell membranes, which have very important physiological roles (*1*). Their structures share a common inositol ring bearing one, two, or three phosphate groups, and their glycerol moieties link both a saturated and an unsaturated alkyl chain. Phosphatidylinositol (*4*, *5*) bisphosphate [$PI(4,5)P_2$ or $PIP_2$][1] is the most abundant phosphoinositide at the plasma membrane and has the ability to interact with a wide range of proteins (*2*−*4*). It is now well documented that $PIP_2$ regulates cytoskeleton−plasma membrane interactions, membrane trafficking, exocytosis, endocytosis, and the activation of enzymes (*2*, *5*−*7*). While it is mostly located at the inner leaflet of the plasma membrane, $PIP_2$ is also present in the nucleus (*8*).

Of the proteins involved in the linkage between components of the cytoskeleton and the plasma membrane, the proteins of the ezrin, radixin, moesin (ERM) family are recognized as being important regulators in the connection between membrane proteins and the cytoskeleton (*9*−*11*). ERM proteins are organized in three distinct domains: (i) the N-terminal membrane-binding domain, which is shared by the ERM proteins and by protein 4.1 and is termed the FERM domain (*9*), (ii) an α-helical domain, and (iii) the C-terminal actin-binding domain. Ezrin, one member of this family, is largely found in intestinal microvilli and in filopodia (*12*).

Within the cell, ezrin can exist in two different states, either dormant or inactive, when the N- and C-terminal domains are tightly associated, thereby masking the F-actin and membrane binding sites (via intra- or intermolecular association) (*13*), or open, i.e., active, when the N-terminus is accessible for membrane binding and the C-terminus is accessible for actin binding. The activation of ezrin requires separation of the N- and C-terminal domains, a process that is dependent on binding with $PIP_2$ at the membrane (*9*, *14*). It is followed by phosphorylation of the threonine 567 residue in the C-terminal domain, resulting in a conformational change in the protein and its subsequent binding to F-actin (*14*, *15*). The FERM domain consists of three lobes (F1, F2, and F3). Experimental evidence showing that the lysine pairs located in subdomains F1 and F3 of the ezrin FERM domain play an important role in the binding of ezrin to multilamellar vesicles containing $PIP_2$ has been obtained (*14*). In addition, the crystal structure of the radixin FERM domain complexed with $IP_3$, the polar head of $PIP_2$ (*16*), suggests the presence of a basic cleft located between subdomains F1 and F3. Both sites are likely to contribute to the binding of the FERM domain to $PIP_2$.

Ezrin in vivo is found mostly as monomers but also exists as oligomers (*17*). The formation of ezrin oligomers has been the subject of only a few in vivo and in vitro studies. Ezrin purified

[†]This work was supported by an ANR PCV 2008 grant to C.P. and L. R. C.P. is a Junior Member of the Institut Universitaire de France whose support is gratefully acknowledged.

*To whom correspondence should be addressed. C.P.: e-mail, Catherine.Picart@minatec.grenoble-inp.fr; phone, 33-(0)456 52 93 11; fax, 33-(0)456 52 93 11. L.R.: e-mail, Laurence.ramos@univ-montp2.fr; phone, 33-(0)4 67 14 42 84; fax, 33-(0)4 67 14 46 37.

[1]Abbreviations: DSP, dithiobis(succinimidyl propionate); DTT, dithiothreitol; DMSO, dimethyl sulfoxide; ERM, ezrin, radixin, moesin; GUVs, giant unilamellar vesicles; $IP_3$, inositol triphosphate; LUVs, large unilamellar vesicles; MES, 2-(*N*-morpholino)ethanesulfonic acid; $PIP_2$, phosphatidylinositol 4,5-bisphosphate; POPC, 1-palmitoyl-2-oleoyl-*sn*-glycero-3-phosphatidylcholine; SDS, sodium dodecyl sulfate; WT ezrin, wild-type ezrin.

 Published on Web 09/27/2010 © 2010 American Chemical Society

from placenta is known to exist both as a monomer and as a dimer (*18*), and oligomers are major cytoskeletal components of placental microvilli (*17*). Stimulation of human A431 cancer cells with epidermal growth factor induces the rapid formation of oligomers in vivo (*14*). The role of the phosphorylation of T567 (mimicked by the T567D mutant) was investigated and is thought to regulate the transition from membrane-bound oligomers to active monomers (*19*), suggesting that the active ezrin linker is a monomer. In addition, in gastric parietal cells, the oligomers are thought to be the membrane-bound dormant form of ezrin (*20*). In vitro experiments evidenced that the T567D mutation has a minor effect on the biochemical activation of ezrin and that the coiled-coil region does not drive dimer formation (*21*). However, the roles of ezrin oligomers are yet to be clarified. Moreover, until now, the role of $PIP_2$ in the formation and stabilization of ezrin oligomers has never been investigated.

A survey of the literature shows that interactions of proteins with $PIP_2$ were studied in vitro using either $PIP_2$ inserted into biomimetic membranes such as large unilamellar vesicles ($PIP_2$ LUVs) (*22*, *23*), giant unilamellar vesicles ($PIP_2$ GUVs) (*24*, *25*) and supported bilayers (*26*, *27*), or $PIP_2$ directly introduced into solution (*28*−*30*). In our study, we investigated the interactions of full-length ezrin and of the ezrin FERM domain with $PIP_2$, which was directly introduced into solution without any other lipids. We also compare data obtained with wild-type ezrin and with an ezrin mutant.

This paper is organized as follows. Using a combination of fluorescence spectroscopy, isothermal titration calorimetry, and proteolysis experiments, we will first show that a conformational change in ezrin is induced by the interaction of ezrin with the entire $PIP_2$ molecule, while no conformational change is detected if $PIP_2$ interacts solely with the FERM domain. Such conformational change does not occur when only the polar headgroup of the $PIP_2$ molecule ($IP_3$) is present, or when the length of the acyl chains of synthetic $PIP_2$ analogues is too short. We found that $PIP_2$ interacts with the FERM domain but does not induce a substantial conformational change in the FERM domain. In addition, we will provide experimental evidence that $PIP_2$ induces the formation of multimers of wild-type ezrin, which represent a small but non-negligible fraction of the total protein. We will also compare the experimental data obtained with wild-type ezrin to those obtained with an ezrin mutant, which had previously been shown not to be localized at the cell plasma membrane. We will discuss our results in terms of the possible sites of interaction of $PIP_2$ with ezrin.

## EXPERIMENTAL PROCEDURES

*Materials*. The sodium salt of L-α-phosphatidylinositol (*4*, *5*) bisphosphate ($PIP_2$) was purchased from Lipid Products (Surrey, Great Britain). $PIP_2$ is extracted from a natural source and thus contains both unsaturated and saturated acyl chains. Synthetic $PIP_2$ analogue molecules with various alkyl chain lengths (C16, C8, and C4), and the polar head of $PIP_2$, inositol triphosphate ($IP_3$), were purchased from Echelon Bioscience. Monoclonal antibodies ($IgG_{2B}$) against $PIP_2$ were purchased from Assay Designs (Ann Arbor, MI). Dimethyl sulfoxide (DMSO), dithiothreitol (DTT), and sodium dodecyl sulfate (SDS) were purchased from Sigma (St. Louis, MO). 1-Palmitoyl-2-oleoyl-*sn*-glycero-3-phosphatidylcholine (POPC) was obtained from Avanti Polar Lipids (Alabaster, AL). Ezrin (wild type and mutant) was kept at 4 °C in a buffer containing 70 mM NaCl and 25 mM 2-(*N*-morpholino)ethanesulfonic acid (MES) at pH 6.2 (MES-NaCl buffer). For the experiments, the buffer was brought to pH 7.4 with 30 mM Tris (MES-Tris-NaCl buffer containing 0.5 mM EGTA, hereafter called ezrin buffer). The FERM domain was kept at 4 °C in a buffer containing 20 mM Tris at pH 7.4

*Ezrin Production and Purification*. The expression and purification of wild-type (WT) ezrin and of the ezrin FERM domain (residues 1−333) cloned in the pGEX 2-T vector have already been described (*31*). The expression of a full-length ezrin mutant possessing six lysine residue mutations (K63N, K64N, K253N, K254N, K262N, and K263N) introduced into the pGEX-2T vector has also been described previously (*14*). This 6N ezrin mutant was found not to interact with large unilamellar vesicles made of a mixture of POPC and $PIP_2$ ($PIP_2$ LUVs) (SI Figure 1 of the Supporting Information) and not to be localized at the membrane of epithelial cells (*14*). Both wild-type ezrin and the ezrin mutant were obtained using the same purification procedure. Of note, the ezrin 6N mutant had been designed on the basis of the analysis of the primary structure of ezrin prior to the determination of the structure of the radixin FERM domain by Hamada et al. (*16*). The structural data provided by Hamada et al. evidenced the presence of a binding site for $IP_3$ (the headgroup of $PIP_2$) located between lobes F1 and F3, which contains a "basic cleft" (K278, R273, R275, and R279). These four residues differ from the residues mutated by Barret et al. (*14*).

*Intrinsic Fluorescence of Tryptophan*. The intrinsic fluorescence of the tryptophan residues in full-length ezrin and in the FERM domain was measured using a fluorescence spectrometer (Series 2 luminescence spectrometer, SLM-Aminco Inc., Northampton, MA). The excitation wavelength was set at 292 ± 2.5 nm, and the emission was acquired over 300−400 nm. The ezrin (wild type and mutant) concentration was fixed at 1 μM and the FERM domain concentration at 7.5 μM. Experiments were performed at least four times on two independent protein preparations.

*Chemical Cross-Linking with DSP*. To cross-link ezrin, dithiobis(succinimidyl propionate) (DSP) (Pierce Chemical Co., Rockford, IL), a homobifunctional thiol-cleavable cross-linker, was used as previously described (*18*). Aliquots (30 μL) from each sample were incubated for 15 min at room temperature in dimethylformamide into which DSP was dissolved at a concentration of 4 mM. The reactions were stopped when the mixtures were boiled in Laemmli sample buffer under nonreducing conditions. In all experiments, the final concentration of dimethylformamide was less than 5%.

*Western Blot*. Ezrin was put into contact with $PIP_2$ in solution. The concentration of ezrin was fixed at 4 μM, and the concentration of $PIP_2$ varied between 0 and 30 μM. After a 15 min incubation of ezrin with $PIP_2$ in solution, 20 μL of these samples was analyzed on a 10% SDS−PAGE gel and then transferred to an Immobilon-P transfer membrane (Millipore, Molsheim, France) using a semidry electroblotter (Integrated Separation Systems, Hyde Park, MA). The blots were blocked with 5% nonfat dry milk and probed directly with an anti-NTER antibody (custom-made gift from C. Roy) and a peroxidase-conjugated anti-$PIP_2$ (Assay Designs). All blots were developed by enhanced chemiluminescence. In some experiments, the blots were stripped according to the manufacturer's instructions and then reprobed with other reagents.

*Proteolysis*. Ezrin at 4 μM was incubated at room temperature in the presence of 0.14 μM chymotrypsin (Boehringer, Mannheim, Germany) in a buffer containing 20 mM Tris-HCl

(pH 7.4), 0.1 mM EDTA, and 15 mM mercaptoethanol (final volume of 30 $\mu$L), in the presence or absence of $PIP_2$. The reaction was stopped by addition of 1 mM phenylmethanesulfonyl fluoride. Fractions were analyzed by gel electrophoresis, blotting, and reaction with a polyclonal antibody raised against the purified recombinant N-terminal domain of ezrin as previously described (*32*).

*Isothermal Titration Calorimetry* (*ITC*). The sample cell was loaded with ~1.4 mL of ezrin at 5 $\mu$M or the FERM domain at 4 $\mu$M. The reference cell contained the ezrin buffer. Titrations were conducted using a 400 $\mu$L syringe filled with a $PIP_2$ solution at 90 $\mu$M in ezrin buffer while the contents were stirred at 300 rpm. Injections were started after the baseline stability had been achieved. A titration experiment consisted of 28 consecutive injections of 10 $\mu$L for a duration of 20 s at 5 min intervals. To correct for the heat effects of the $PIP_2$ solution, control experiments were performed by injection of $PIP_2$ into the ezrin buffer. The heat released by dilution of the $PIP_2$ in the cell was negligible. The resulting data were fitted to a one-binding site model using MicroCal ORIGIN software supplied with the instrument. The standard molar enthalpy change for binding ($\Delta H$) and the binding constant ($K$) were determined. The standard molar free energy change ($\Delta G$) and the standard molar entropy change ($\Delta S$) for the binding reaction were calculated by the fundamental equations of thermodynamics:

$$\Delta G = -RT \ln K$$

$$\Delta S = \frac{\Delta H - \Delta G}{T}$$

Three independent titrations on two different ezrin and FERM domain batches were performed.

*Light Scattering*. Light scattering measurements were taken on a standard setup. The sample was placed at the center of a thermostated AMTEC goniometer and was illuminated with an argon ion laser (514.5 nm). A Brookhaven BI9400 correlator was used to calculate the normalized time autocorrelation function of the scattered intensity. The scattering angle varied between 50° and 110°. The size distribution of the scatterers was determined by fitting the time correlation function using the non-negative least-squares (NNLS) method. The ezrin concentration was fixed at 12.5 $\mu$M. The $PIP_2$ concentrations varied between 0 and 40 $\mu$M. Before the measurement, the solutions were filtered through a polycarbonate membrane with a pore size of 0.22 $\mu$m. The duration of one measurement at one given scattering angle was ~20 min.

## RESULTS

We investigated ezrin−$PIP_2$ interactions when the $PIP_2$ concentration in buffer varied from 0 to 40 $\mu$M. Because $PIP_2$ molecules are believed to self-assemble in micelles at concentrations larger than a critical micellar concentration (cmc), we first verified the state of $PIP_2$ molecules in the ezrin buffer. In the literature, the cmc of $PIP_2$ in several low-ionic strength buffers has been evaluated using different techniques. Values for the cmc ranged between 10 and 60 $\mu$M (*30*, *33*). Results obtained via static and dynamic light scattering under our experimental conditions (ezrin buffer containing 70 mM NaCl) indicated that no micelle was present (SI Figure 2 of the Supporting Information) and thus that the $PIP_2$ was dispersed in a unimolecular fashion.

*Interaction of $PIP_2$ with Full-Length Ezrin and with the FERM Domain*. Isothermal titration calorimetry (ITC) was used to investigate the interactions between $PIP_2$ and full-length ezrin and between $PIP_2$ and the FERM domain of ezrin. Figure 1 shows the heat exchange measured for each injection of $PIP_2$ into the ITC sample cell containing a solution of ezrin (Figure 1A) and a solution of FERM domain (Figure 1B). The binding curves obtained from a plot of the heats (from each injection) against the molar ratio of $PIP_2$ to ezrin (and of $PIP_2$ to the FERM domain) are shown in panels C and D of Figure 1, respectively. They confirm that the $PIP_2$ molecules interact with both full-length ezrin and the FERM domain. The experiments demonstrate, however, very distinct behaviors of the two species. The interaction of $PIP_2$ with full-length ezrin was endothermic (Figure 1C), while the interaction with the FERM domain was exothermic (Figure 1D). We measured a $\Delta H$ of $12 \pm 4$ kJ/mol for ezrin and a $\Delta H$ of $-6 \pm 2$ kJ/mol for the FERM domain [these values correspond to three independent measurements (mean ± standard deviation) performed on two different protein batches]. The entropic contribution was favorable in both cases, as $T\Delta S$ was positive: $T\Delta S = 48 \pm 8$ kJ/mol for ezrin, and $T\Delta S = 30 \pm 3$ kJ/mol for the FERM domain. Interestingly, the free energies ($\Delta G = \Delta H - T\Delta S$) of the interaction are on the same order of magnitude for ezrin and the FERM domain. We find $\Delta G = -36 \pm 12$ kJ/mol for ezrin and $\Delta G = -36 \pm 5$ kJ/mol for the FERM domain. Interestingly, the dissociation constants ($K_d = 1/K$) are therefore on the same order of magnitude for full-length ezrin and for the FERM domain, ~0.4−0.6 $\mu$M. Additional experiments (intrinsic fluorescence spectroscopy and mild proteolysis) were performed to elucidate further the contrasted behavior of full-length ezrin and the FERM domain despite similar affinities with $PIP_2$.

*$PIP_2$ Induced a Conformational Change in Full-Length Ezrin*. We show in Figure 2A the evolution of the fluorescence emission spectra of wild-type ezrin upon addition of $PIP_2$ at increasing concentrations. In these experiments, the protein concentration was fixed at 1 $\mu$M and the $PIP_2$ concentration varied between 0 and 40 $\mu$M. We observed that the fluorescence intensity strongly decreased when the $PIP_2$ concentration increased, while the position of the peak of fluorescence intensity (at ~336 nm) did not vary significantly. In Figure 2B, the percentage of the decrease in fluorescence (taken at the peak of the fluorescence signal), also called quenching, is plotted as a function of the $PIP_2$ concentration. A hyperbola-like increase in quenching was measured, with a maximum quenching of 54 ± 8%. For comparison, we also measured the quenching for the interaction of ezrin with different synthetic derivatives of $PIP_2$ with various alkyl chain lengths of 16, 8, and 4 carbons (called C16-$PIP_2$, C8-$PIP_2$, and C4-$PIP_2$, respectively). The effects of $IP_3$, the polar headgroup of $PIP_2$, an inert lipid, POPC, and a standard surfactant, SDS, were also measured. Figure 1C displays the quenching of these different compounds when their concentration is 40 $\mu$M, which corresponds to the plateau value. Interestingly, while the decrease in fluorescence reached 54 ± 8% for native $PIP_2$, the maximum quenching was approximately half of this value for C16-$PIP_2$. The C8-$PIP_2$ was slightly above the noise, which was estimated to be ~10%. Values for $PIP_2$ analogues with shorter chains as well as for $IP_3$, POPC, and SDS were within the noise value. Thus, the effect of $PIP_2$ was significantly more pronounced than the effect of all the other species.

Measurements were also performed with the ezrin 6N mutant that contains six mutations of lysine residues, all located in the FERM domain (K63N, K64N, K253N, K254N, K262N, and

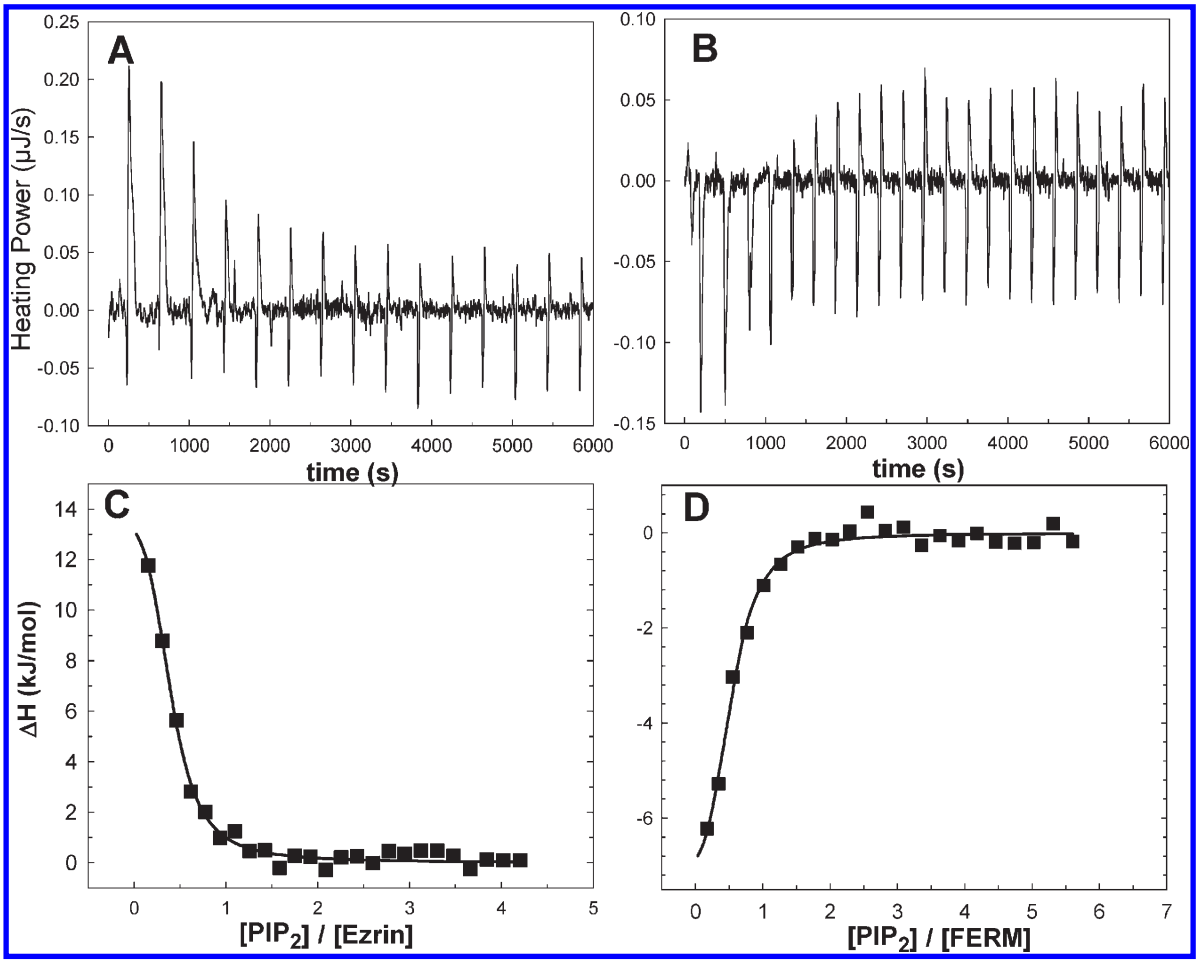


FIGURE 1: Isothermal titration calorimetry experiments of the interaction of ezrin (A and C) and the FERM domain (B and D) with native $PIP_2$. Raw data for sequential 10 $\mu$L injections of 90 $\mu$M $PIP_2$ into a solution of ezrin at 5 $\mu$M (A) and of the FERM domain at 4 $\mu$M (B). Titration curves, heat observed on each injection vs the molar ratio of $PIP_2$ to ezrin (C) and $PIP_2$ to the FERM domain (D). Data were fitted to a one-binding site model. Symbols are experimental data, and lines represent the best fit. The interaction with $PIP_2$ was exothermic for ezrin and endothermic for the FERM domain.

K263N) (*14*). A significant quenching, comparable to that measured for wild-type ezrin, was also measured (Figure 2B,D). However, a major difference is that the binding curve of $PIP_2$ with WT ezrin follows a hyperbolic trend, which is typical of specific interactions, whereas that of $PIP_2$ with the ezrin 6N mutant cannot be fitted by a hyperbolic function. Instead, the quenching appears roughly proportional to the concentration of $PIP_2$. This type of binding curve is typical for nonspecific interactions. This result will be discussed in the next section.

As the quenching observed here for full-length ezrin is not associated with a change in the maximum of the emission spectrum and to rule out the possibility that the simple binding of $PIP_2$ may change the tryptophan fluorescence intensity, we also measured the intrinsic fluorescence of the FERM domain in the presence of $PIP_2$. The quenching of FERM as a function of $PIP_2$ concentration is shown together with the data for full-length ezrin in Figure 2B. Although the shapes of the curves are similar in the two cases, the absolute values of the quenching are much weaker for the FERM domain. We indeed measured a much lower maximum quenching for the FERM domain (21 $\pm$ 3%) than for full-length ezrin (54 $\pm$ 8%) (Figure 2B,C). This suggests that the trend observed for the intrinsic fluorescence of full-length ezrin is not uniquely due to a change in tryptophan fluorescence upon binding of $PIP_2$ to the FERM domain. Instead, it may be ascribed to a conformational change in ezrin.

To confirm the effect of $PIP_2$ on the conformation of ezrin, we verified the sensitivity of ezrin to mild proteolysis using chymotrypsin (*14*). Figure 3A follows the degradation of ezrin over 90 min after the addition of the enzyme. This was compared with experiments in which $PIP_2$ was introduced 5 min after the enzyme (Figure 3B). Chymotrypsin was found to degrade ezrin in ~90 min (Figure 3A). However, the presence of $PIP_2$ added at early times noticeably increased the level of ezrin proteolysis. Indeed, after only 5 min, major degradation products of ezrin with a molecular mass of < 24 kDa were visible (Figure 3B). The enhanced sensitivity of ezrin to proteolysis in the presence of $PIP_2$ is in agreement with a $PIP_2$-induced conformational change of the ezrin that will render the whole protein more accessible to the enzyme. This result is in agreement with the intrinsic fluorescence spectroscopy measurements. Similarly, the degradation of the FERM domain [band visible at ~35 kDa (*14*)] was enhanced in the presence of $PIP_2$: intact FERM was still present after incubation for more than 90 min with chymotrypsin, whereas the degradation of the FERM domain was completed after less than 60 min in the presence of $PIP_2$.

*$PIP_2$ Induced the Formation of Ezrin Multimers*. The size of ezrin in solution was investigated by dynamic light scattering measurements. We show in Figure 4A the correlation function for ezrin in buffer, which can be well fitted with a decaying monoexponential functional form, with a unique characteristic

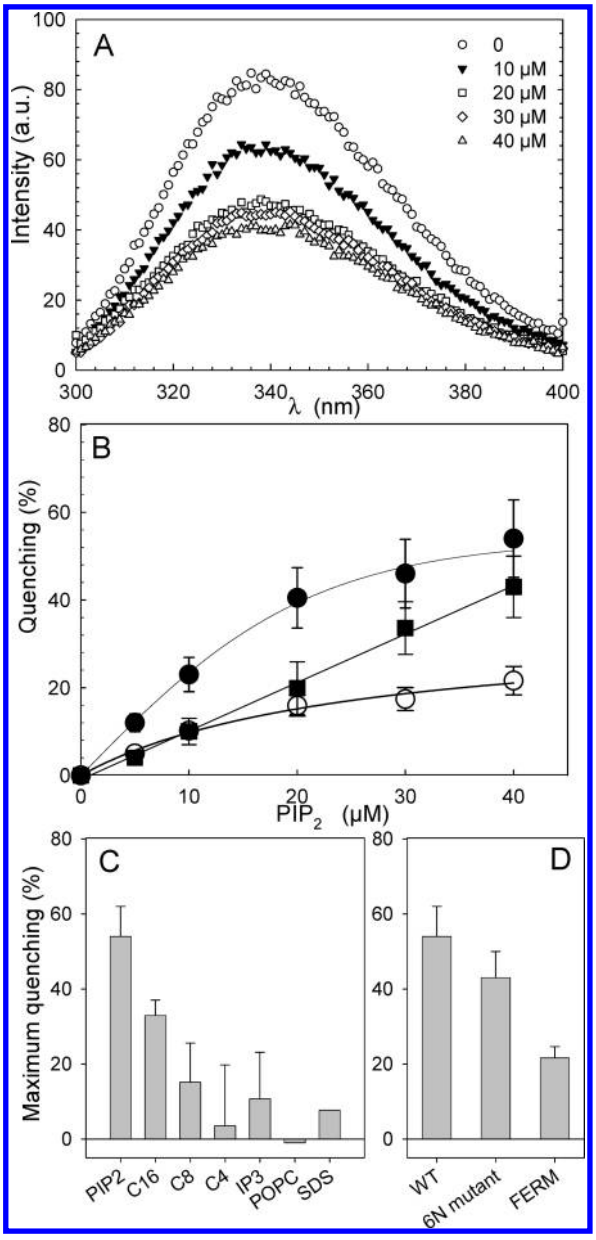


FIGURE 2: (A) Emission fluorescence spectra of wild-type ezrin (1 $\mu$M) in the presence of native $PIP_2$ in solution (from 0 to 40 $\mu$M) as indicated in the legend. (B) Relative decrease in the maximum fluorescence emission, as a function of $PIP_2$ concentration, as deduced from the spectra shown in panel A for wild-type ezrin (●) and for the ezrin FERM domain (○). The data for the ezrin 6N mutant are also plotted (■). Data are means ± the standard deviation of three independent experiments performed on one protein batch. For wild-type ezrin and FERM domain data, the lines are hyperbolic fits of the experimental results, and for ezrin 6N mutant data, the line is a linear fit of the experimental results. (C) Maximum quenching for wild-type ezrin in the presence of native $PIP_2$, synthetic $PIP_2$ analogues with different acyl chain lengths (16, 8, and 4), $IP_3$, the polar head of $PIP_2$, POPC, and SDS. (D) Maximum quenching measured for WT ezrin as compared to the FERM domain (ezrin 1−333) and to the ezrin 6N mutant in the presence of native $PIP_2$. In this latter case, the value of quenching at 40% $PIP_2$ was plotted as no plateau was observed. Data are means ± the standard deviation four independent experiments performed on two different protein batches.

time, $\tau$. We measured that $\tau$ is inversely proportional to wave vector $q$ (SI Figure 3 of the Supporting Information). From the slope, we derived the hydrodynamic diameter, $D_H$, of the scattering object. We found $D_H = 8.0 \pm 0.2$ nm, in good agreement with previous estimates of the ezrin diameter determined by gel filtration (*21*) and by fluorescence correlation spectroscopy (*34*). In the presence of $PIP_2$, the overall decrease in the correlation function slowed and the data could no longer be fitted with a simple exponential form (Figure 4A). This indicates the presence of more than one characteristic time, hence of more than one species in solution. Panels B and C of Figure 4 show the size distribution in intensity extracted from the correlation functions for ezrin alone (Figure 4B) and for ezrin interacting with $PIP_2$ (Figure 4C). With or without $PIP_2$, a peak around 6−12 nm was systematically identified, which corresponds to ezrin in the monomeric form. In the presence of $PIP_2$, a bimodial distribution is measured: larger species, whose average sizes range from ~20 nm for a $PIP_2$ concentration of 5 $\mu$M to ~30 nm for a $PIP_2$ concentration of 40 $\mu$M, coexist with monomeric ezrin. The diameter of the different species in solution is represented as a function of the $PIP_2$ concentration in Figure 4D. We further verified that the $PIP_2$ alone in solution did not give any measurable correlation functions (data not shown) over the whole range of $PIP_2$ concentrations investigated. The larger species can thus be identified as ezrin oligomers.

We performed Western blot assays to confirm that $PIP_2$ induced the formation of ezrin oligomers. For comparison, we also investigated the behavior of the ezrin 6N mutant. We employed a protocol already established by Bretscher (*18*), which makes use of a homobifunctional reagent, DSP, to chemically cross-link ezrin multimers. Solutions of wild-type ezrin or the ezrin 6N mutant in the interaction with $PIP_2$ were analyzed by Western blotting using either an antibody raised against the N-terminal domain of ezrin (Figure 5A,C) or anti-$PIP_2$ antibodies (Figure 5B,D). Under control conditions (no $PIP_2$ in solution), only ezrin monomers were present as just a single band was detected (Figure 5A, left band). Interestingly, an intense band corresponding to a higher molecular mass was detected in the presence of $PIP_2$, when the anti-N-terminal antibody was used. This band may be attributed to a dimer of ezrin as its molecular mass is ~120 kDa. The formation of ezrin oligomers was better visualized when the cross-linker DSP was used. As shown by the broad bands in panels A and B of Figure 5, ezrin oligomers with higher molecular masses were formed (~180−220 kDa) that also contained $PIP_2$. This qualitatively proved that $PIP_2$ was irreversibly linked to ezrin oligomers.

For the ezrin 6N mutant, the Western blot confirmed that $PIP_2$ interacts with the mutant, as $PIP_2$ was immunodetected at a molecular mass equal to that of ezrin (Figure 5D). However, very interestingly, only ezrin monomers were formed as a single band was detected with the anti-N-terminal antibody (Figure 5C). This demonstrates the crucial role of the mutated amino acids in the formation of ezrin oligomers.

## DISCUSSION

*Interaction of $PIP_2$ with Full-Length Ezrin and with the FERM Domain*. Binding affinities of full-length ezrin and of the FERM domain of ezrin were determined using ITC. Similar values for the dissociation constant, $K_d$, between 0.4 and 0.6 $\mu$M, were measured for the two species. It is, to the best of our knowledge, the first experimental determination of the affinity between $PIP_2$ and the FERM domain. Similar values for the FERM domain and ezrin could be expected because $PIP_2$ interacts solely with the FERM domain. However, similar values for the FERM domain and ezrin show also that the interactions between $PIP_2$ and the FERM domain are not hindered in full-length ezrin. This is a new and valuable piece of information.

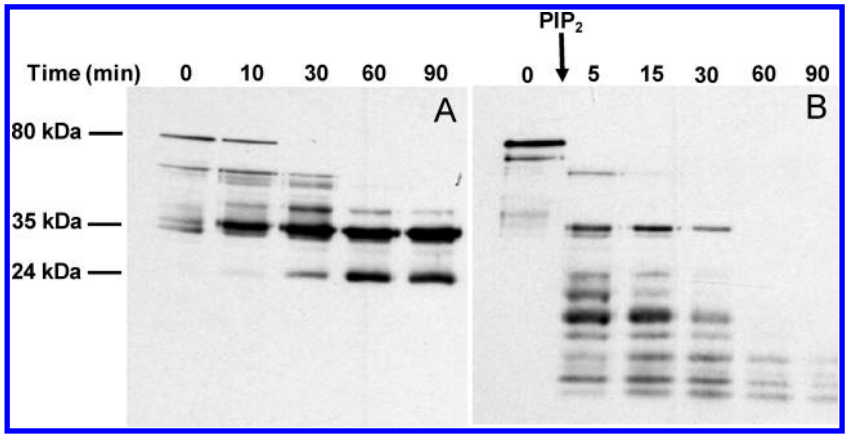


FIGURE 3: Effect of chymotrypsin on the degradation of ezrin in the presence (A) or absence (B) of $PIP_2$. The ezrin concentration was 4 $\mu$M, and the chymotrypsin concentration was 0.14 $\mu$M. In the absence of $PIP_2$ (A), ezrin was resistant for at least 30 min after the addition of chymotrypsin. (B) When 45 $\mu$M $PIP_2$ was added, the protein was rapidly degraded and degradation products with smaller molecular masses are detected after only 5 min. There was no protein left 90 min after $PIP_2$ addition.

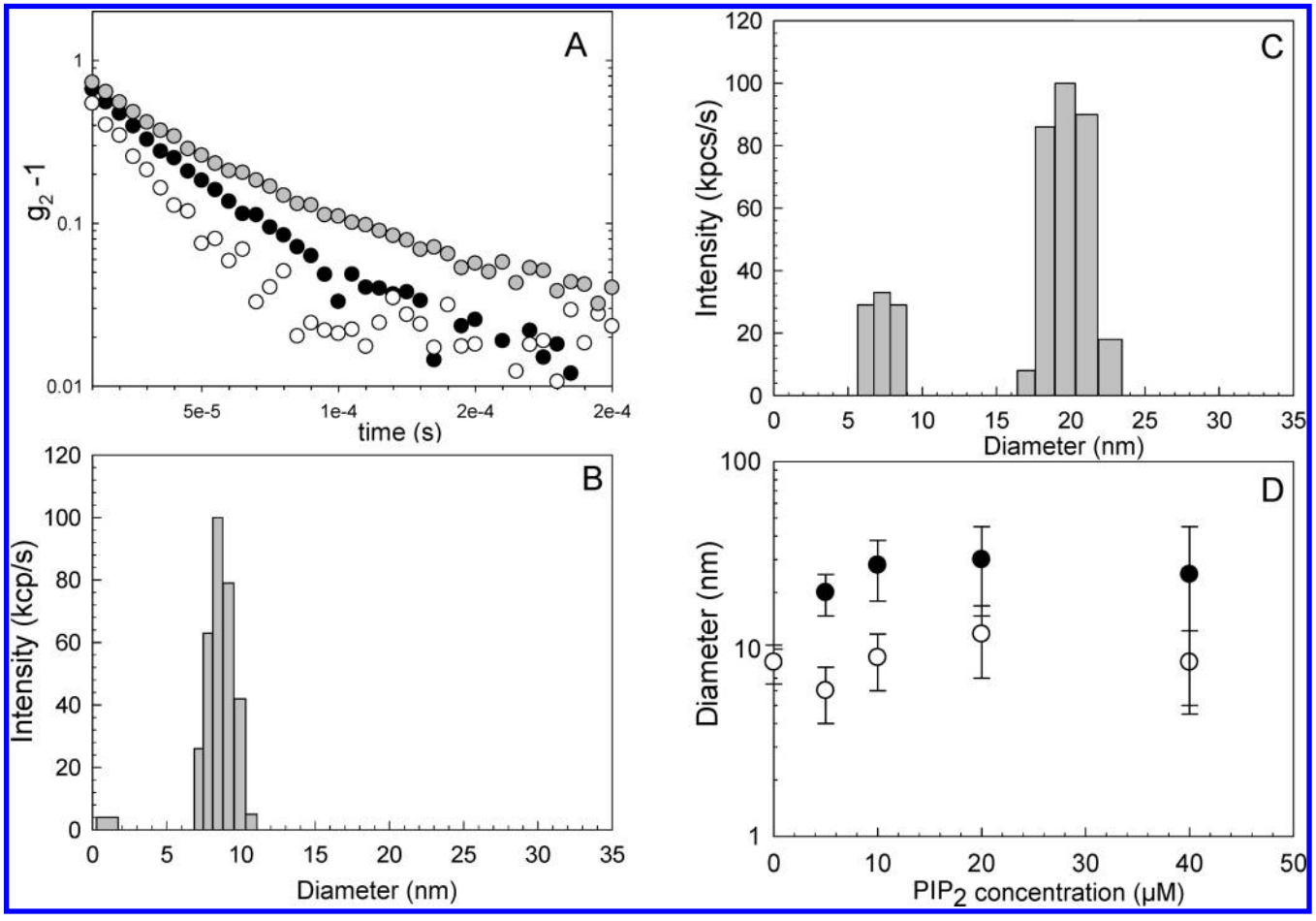


FIGURE 4: DLS measurements on ezrin in the absence and presence of $PIP_2$ at increasing concentrations. (A) Correlation function of WT ezrin alone (12 $\mu$M) (white circles) or in the presence of $PIP_2$ at 5 (black circles) and 10 $\mu$M (gray circles). The correlation function shifted to the right in the presence of $PIP_2$, indicating the presence of species larger than ezrin monomers. Size distribution of the species in solution, for ezrin alone (B) and for ezrin with $PIP_2$ at a concentration of 5 $\mu$M (C), as deduced from the correlation functions using the NNLS method. In the absence of $PIP_2$, one species (ezrin monomer, diameter of ~8 nm) was detected, whereas two species were detected (ezrin monomer and ezrin oligomers) in the presence of $PIP_2$. (D) Diameters of the different species in solution as a function of $PIP_2$ concentration. White circles correspond to ezrin monomers and black circles to ezrin oligomers. Errors bars correspond to the width of the size distribution like those shown in panels B and C.

We note, moreover, that the measured dissociation constants were ~1 order of magnitude smaller than those measured previously between full-length ezrin and $PIP_2$ LUVs (*34*). Interactions between ezrin and $PIP_2$ in solution thus appear to be slightly stronger than those between ezrin and $PIP_2$ LUVs. This is consistent with the fact that acyl chains of $PIP_2$ may play a role in the interaction with ezrin as seen in the intrinsic fluorescence of ezrin interacting with $PIP_2$ acyl chain analogues.

*Conformational Changes in Ezrin.* Several experiments were performed to investigate the possible conformational

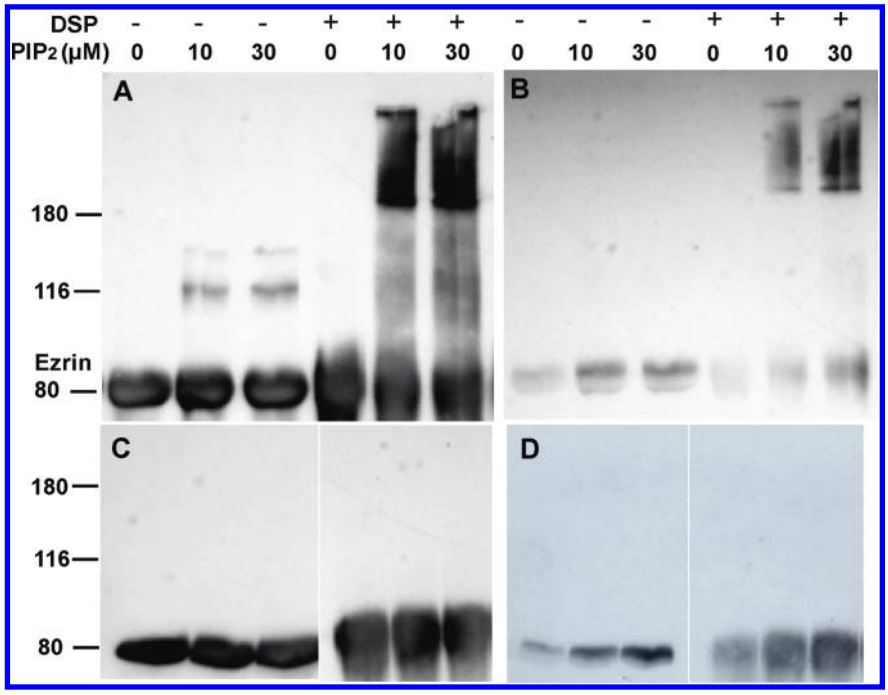


FIGURE 5: Western blot of ezrin (A and B) and the ezrin 6N mutant (C and D) in the presence or absence of $PIP_2$ and in the presence or absence of DSP as a cross-linker. (A) Ezrin immunolabeling with antibodies directed against the N-terminal domain shows the presence of species with higher molecular masses, both with and without the cross-linker. The formation of species with higher molecular masses was dependent on the $PIP_2$ concentration. For the ezrin mutant (C), no large species was present. (B) $PIP_2$ immunolabeling with anti-$PIP_2$ antibodies revealed that the interaction between ezrin and $PIP_2$ was resistant to denaturation by SDS and $PIP_2$ was associated with the high-molecular mass species (B). On the other hand, $PIP_2$ was only detected at the molecular mass of ezrin for the ezrin 6N mutant (D). The dashes indicate the positions in the gel of the molecular mass markers (80, 116, and 180 kDa).

changes experienced by ezrin molecules upon interaction with phosphoinositides and to compare the behavior of full-length ezrin and the FERM domain. Tryptophan fluorescence is sensitive to the polarity of its environment (*35*). In general, a decrease in fluorescence emission indicates that the tryptophans are in a more polar environment. Ezrin possesses seven tryptophan residues; six are located in the FERM domain, and one is located in the coiled coil. Their precise location is shown in Figure 6, where the tryptophan residues have been colored blue. In the dormant state, the C-terminal domain interacts with the N-terminal domain (Figure 6A). In our experiments, the decrease in the fluorescence of full-length ezrin upon addition of $PIP_2$ and the fact that the FERM domain was much less sensitive to $PIP_2$ suggest a conformational change in ezrin, with an opening of the molecule through a disruption of the C-terminal−N-terminal interaction. This would lead to exposure to a more polar environment of the six tryptophan residues located in the FERM domain. Blank measurements performed using POPC and SDS did not show any quenching and thus demonstrated that a specific interaction was probed. Data obtained with the polar head of $PIP_2$ and with $PIP_2$ analogues with shorter acyl chains strongly suggested a role for at least one of the two alkyl chains in the natural $PIP_2$ molecule as the quenching was drastically reduced when the length of the acyl chain diminished.

The structure of the FERM domain (Figure 6B) shows the presence of a hydrophobic pocket, rich in phenylalanine and tryptophan residues. On the basis of this structural observation, differences measured on ezrin for the different $PIP_2$ analogues and for the $PIP_2$ headgroup might be related to interactions of acyl chains with the FERM domain via this hydrophobic pocket. Interestingly, recent experimental studies also attribute a role to $PIP_2$ acyl chains in the interactions of $PIP_2$ with proteins (*36*) (*37*): in particular, data for the interactions between cofilin and synthetic $PIP_2$ analogues also indicated that a minimum acyl chain length was required for the interaction to occur (*36*). Molecular dynamics simulations have also suggested a role for the acyl chains in gelsolin−$PIP_2$ interactions in a model membrane (*37*).

Full-length ezrin is already known to be sensitive to chymotrypsin (*14*). The rate of proteolysis is dependent on the conformational state (more or less compact) of the protein. Importantly, the presence of $PIP_2$ noticeably enhanced the sensitivity of ezrin to chymotrypsin, implying a less compact state of the protein, in agreement with an opening of the protein. This is effectively what was expected from the analysis of the structural changes that occur upon activation (*16*, *38*). Mild proteolysis experiments indicate also a conformational change in the FERM domain in the presence of $PIP_2$. This result is consistent with the quenching data, where a small, as compared to that measured for ezrin, but noticeable quenching has been measured in the case of the FERM domain. This may be related to a slight conformational change in the FERM domain caused by $PIP_2$ binding, as suggested by Hamada et al. (*16*), who determined the structure of the FERM domain of radixin with $IP_3$, the headgroup of $PIP_2$.

Furthermore, the ITC data are also compatible with an opening of full-length ezrin upon interaction with native $PIP_2$. Indeed, our results show that the interaction of $PIP_2$ with the FERM domain is enthalpy-driven, as expected for a charge−charge interaction between the phospholipid headgroups and the FERM domain. Conversely, the interaction between $PIP_2$ and ezrin is driven by favorable entropy, dominating an unfavorable enthalpy contribution. This thermodynamic signature is in agreement with an increase in flexibility obtained through an opening of the ezrin molecule.

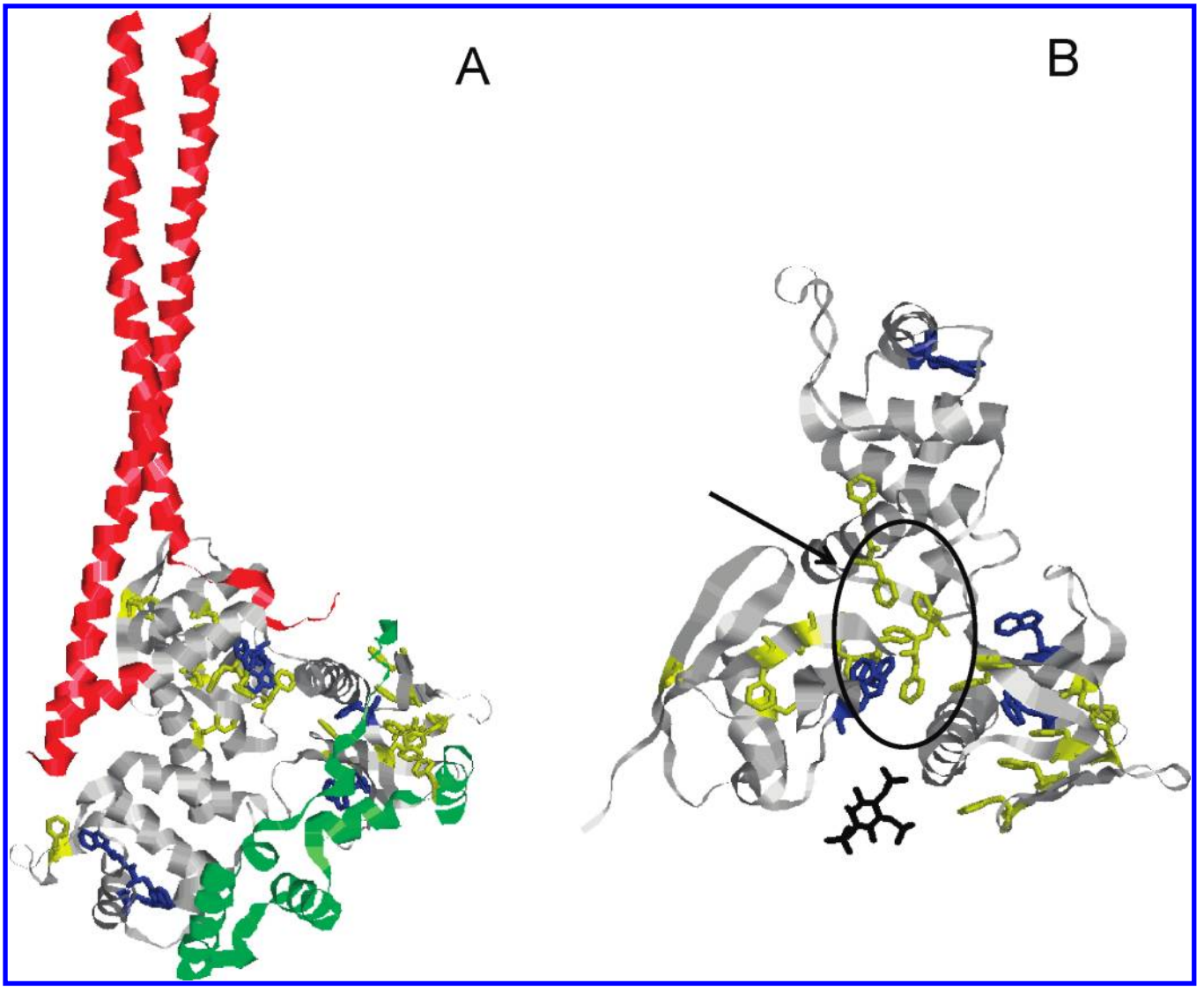


FIGURE 6: Three-dimensional visualization of full-length ezrin (derived from the moesin Protein Data Bank entry 2I1K) and of the ezrin FERM domain (Protein Data Bank entry 1GC6) by Rasmol. (A) Three-dimensional structure of ezrin. The FERM domain is colored gray, the α-helical region red, and the C-terminus green. The tryptophan residues are colored blue and the phenylalanine residues yellow. The C-terminal domain is masking the FERM domain and the tryptophan residues in the FERM domain. (B) Structure of the FERM domain cocrystallized with $IP_3$ (black). The hydrophobic pocket, indicated by an arrow, is represented by a black ellipse.

Overall, our results thus demonstrated that $PIP_2$ interacts with full-length ezrin and induces a conformational change in the protein. Tryptophan data suggested on the other hand that synthetic $PIP_2$ analogues with alkyl chains shorter than those of native $PIP_2$ were not able to induce a complete conformational change in the ezrin.

*Comparison between WT Ezrin and the Ezrin 6N Mutant*. The quenching data show that $PIP_2$ interacted with the 6N ezrin mutant but in a manner different from that with which it interacted with WT ezrin. The results suggested the presence of nonspecific interactions between the mutant and $PIP_2$ and of specific interactions with WT ezrin and $PIP_2$. The very different interaction observed in the case of the 6N ezrin mutant indicates that there might be another binding site for $PIP_2$, distinct from the basic lysine residues identified by Barret et al. (*14*). A good candidate is the basic site proposed by Hamada (*16*), who determined the ezrin FERM domain structure. This basic cleft contains arginine residues (R273, R275, and R279) and a lysine residue (K278); all these residues are different from the residues mutated in this study (see Figure 10 of ref *34* for the visualization of the residues identified by Hamada and of those identified by Barret). Our quenching experiments suggest that this interaction is not specific.

Very interestingly, by determining the structure of full-length (dormant) moesin, Tesmer and co-workers (*39*) have shown that this $IP_3$ binding site is sterically blocked by the linker region in dormant moesin (Figure 7 of ref *39*). Our experiments would thus suggest that this $IP_3$ binding site is unmasked in the 6N ezrin mutant and that $PIP_2$ can interact with the mutant via this basic cleft. Of note, this 6N mutant can interact nonspecifically with $PIP_2$ in solution but cannot interact with $PIP_2$ inserted in the membrane LUVs (SI Figure 1 of the Supporting Information), which also suggests a role for the flexibility and exposure of $PIP_2$ in the interaction. In other words, the phosphate groups of $PIP_2$ may interact slightly differently with ezrin or the ezrin mutant when $PIP_2$ is constrained by neighboring lipids.

On the basis of our data, we therefore propose that the lysine residues located in lobes F1 and F3 (K53, K54, K253, K254, K263, and K264) are those involved in the specific interaction

of ezrin with $PIP_2$ but that other basic residues located in the basic cleft can reinforce this interaction in a nonspecific manner.

*Formation of Ezrin Oligomers and Clusters*. Western blot and DLS data showed the formation of ezrin oligomers during interaction with $PIP_2$ in solution. The size of the oligomers extracted from DLS (diameter between 20 and 30 nm) was compatible with the molecular mass of the oligomers measured in the Western blot. Importantly, the Western blots revealed that the oligomers contained both ezrin and $PIP_2$, which suggests that the interaction is tight and resists the disruption by SDS. Very interestingly, similar findings have already been observed by Nakamura et al. for platelet moesin (*40*). These authors observed a shift in moesin from its normal migration position to slower-migrating species, which was specific to $PIP_2$. Unfortunately, they did not investigate whether $PIP_2$ was associated with moesin. In addition, previous confocal observations (*43*) have shown that the interaction of ezrin with giant unilamellar vesicles made of a mixture of phospholipids, cholesterol, and $PIP_2$ ($PIP_2$ GUVs) led to clusters of $PIP_2$ and ezrin at the membrane of the GUVs. This might be connected with $PIP_2$-induced ezrin multimer formation in solution. In the case of the ezrin 6N mutant, although some interaction was still observed with $PIP_2$ in solution, no oligomer formation was observed. This indicates that the mutated lysine residues in the FERM domain play a crucial role in the formation of ezrin oligomers.

*Possible Relevance in Vivo*. The consequences of the ezrin−$PIP_2$ interactions may be important in vivo. The oligomerization of ezrin has been observed in vivo (*19*, *21*), but the role of $PIP_2$ in this interaction has never been investigated more precisely in vitro. $PIP_2$ is indeed of utmost importance for the localization of ezrin at the plasma membrane. The fact that $PIP_2$ may be primordial for oligomerization highlights the possible role of ezrin during events related to membrane and cytoskeletal morphological changes (*41*). During bleb retraction, for instance, the membrane needs to constantly follow the movement of the cytoskeleton as its movement is not governed by protrusion forces (*42*). A hypothesis is that ezrin may create clusters of $PIP_2$ within the membrane, which has already been seen on $PIP_2$ GUVs (*43*), and like in an the autoamplification loop, $PIP_2$ may induce ezrin oligomerization. Such a process would be a very efficient means of increasing the quantity of ezrin at the membrane−cytoskeleton activity areas.

## CONCLUSIONS

We showed that native $PIP_2$ induced a conformational change in recombinant ezrin and in the FERM domain. By comparing data obtained with full-length ezrin and with a 6N mutant, we suggest that different residues located in the FERM domain are all important in the binding to $PIP_2$ and contribute to the specific and nonspecific interaction of the ezrin with $PIP_2$. Interestingly, $PIP_2$ in solution was able to induce ezrin oligomer formation, a process that was elucidated here for the first time. This process of $PIP_2$-induced oligomer formation in vitro may be related to the formation of oligomers already observed in vivo but whose origin had until now remained unexplained. The possible role of $PIP_2$ in ezrin oligomers may be important for the effective targeting of ezrin at the plasma membrane and its subsequent association with actin filaments during morphogenesis.

## ACKNOWLEDGMENT

We thank Martin In (LCVN, Montpellier, France) for help in the DLS experiments. We also thank Christian Roy (LDIMNP, Montpellier, France), Andrea Parmeggiani (LDIMNP, Montpellier, France), Laurent Blanchoin (CEA, Grenoble, France), and Steve Shaw (National Institutes of Health, Bethesda, MD) for fruitful discussions.

## SUPPORTING INFORMATION AVAILABLE

Cosedimentation assay of the ezrin 6N mutant with $PIP_2$ LUVs (SI Figure 1), scattered intensity as measured by light scattering as a function of the concentration of native $PIP_2$ in ezrin buffer (SI Figure 2), and measurement of the size of ezrin by dynamic light scattering (SI Figure 3). This material is available free of charge via the Internet at http://pubs.acs.org.

## REFERENCES

1. Payrastre, B., Missy, K., Giuriato, S., Bodin, S., Plantavid, M., and Gratacap, M. (2001) Phosphoinositides: Key players in cell signalling, in time and space. *Cell. Signalling 13*, 377–387.
2. Yin, H. L., and Janmey, P. A. (2003) Phosphoinositide regulation of the actin cytoskeleton. *Annu. Rev. Physiol. 65*, 761–789.
3. Ling, K., Schill, N. J., Wagoner, M. P., Sun, Y., and Anderson, R. A. (2006) Movin' on up: The role of $PtdIns_{4,5}P_2$ in cell migration. *Trends Cell Biol. 16*, 276–284.
4. Niggli, V. (2005) Regulation of protein activities by phosphoinositide phosphates. *Annu. Rev. Cell Dev. Biol. 21*, 57–79.
5. Martin, T. F. (2001) $PI_{4,5}P_2$ regulation of surface membrane traffic. *Curr. Opin. Cell Biol. 13*, 493–499.
6. Simonsen, A., Wurmser, A. E., Emr, S. D., and Stenmark, H. (2001) The role of phosphoinositides in membrane transport. *Curr. Opin. Cell Biol. 13*, 485–492.
7. McLaughlin, S., and Murray, D. (2005) Plasma membrane phosphoinositide organization by protein electrostatics. *Nature 438*, 605–611.
8. Mazzotti, G., Zini, N., Rizzi, E., Rizzoli, R., Galanzi, A., Ognibene, A., Santi, S., Matteucci, A., Martelli, A. M., and Maraldi, N. M. (1995) Immunocytochemical detection of phosphatidylinositol 4, 5-bisphosphate localization sites within the nucleus. *J. Histochem. Cytochem. 43*, 181–191.
9. Bretscher, A., Edwards, K., and Fehon, R. G. (2002) ERM proteins and merlin: Integrators at the cell cortex. *Nat. Rev. Mol. Cell Biol. 3*, 586–599.
10. Mangeat, P., Roy, C., and Martin, M. (1999) ERM proteins in cell adhesion and membrane dynamics. *Trends Cell Biol. 9*, 187–192.
11. Tsukita, S., and Yonemura, S. (1999) Cortical actin organization: Lessons from ERM (ezrin/radixin/moesin) proteins. *J. Biol. Chem. 274*, 34507–34510.
12. Yonemura, S., and Tsukita, S. (1999) Direct involvement of ezrin/radixin/moesin (ERM)-binding membrane proteins in the organization of microvilli in collaboration with activated ERM proteins. *J. Cell Biol. 145*, 1497–1509.
13. Gary, R., and Bretscher, A. (1995) Ezrin self-association involves binding of an N-terminal domain to a normally masked C-terminal domain that includes the F-actin binding site. *Mol. Biol. Cell 6*, 1061–1075.
14. Barret, C., Roy, C., Montcourrier, P., Mangeat, P., and Niggli, V. (2000) Mutagenesis of the phosphatidylinositol 4,5-bisphosphate ($PIP_2$) binding site in the $NH_2$-terminal domain of ezrin correlates with its altered cellular distribution. *J. Cell Biol. 151*, 1067–1080.
15. Simons, P. C., Pietromonaco, S. F., Reczek, D., Bretscher, A., and Elias, L. (1998) C-terminal threonine phosphorylation activates ERM proteins to link the cell's cortical lipid bilayer to the cytoskeleton. *Biochem. Biophys. Res. Commun. 253*, 561–565.
16. Hamada, K., Shimizu, T., Matsui, T., Tsukita, S., and Hakoshima, T. (2000) Structural basis of the membrane-targeting and unmasking mechanisms of the radixin FERM domain. *EMBO J. 19*, 4449–4462.
17. Berryman, M., Gary, R., and Bretscher, A. (1995) Ezrin oligomers are major cytoskeletal components of placental microvilli: A proposal for their involvement in cortical morphogenesis. *J. Cell Biol. 131*, 1231–1242.
18. Bretscher, A., Gary, R., and Berryman, M. (1995) Soluble ezrin purified from placenta exists as stable monomers and elongated dimers with masked C-terminal ezrin-radixin-moesin association domains. *Biochemistry 34*, 16830–16837.

19. Gautreau, A., Louvard, D., and Arpin, M. (2000) Morphogenic effects of ezrin require a phosphorylation-induced transition from oligomers to monomers at the plasma membrane. *J. Cell Biol. 150*, 193–203.
20. Zhu, L., Liu, Y., and Forte, J. G. (2005) Ezrin oligomers are the membrane-bound dormant form in gastric parietal cells. *Am. J. Physiol. 288*, C1242–C1254.
21. Chambers, D. N., and Bretscher, A. (2005) Ezrin mutants affecting dimerization and activation. *Biochemistry 44*, 3926–3932.
22. Wang, J., Gambhir, A., Hangyas-Mihalyne, G., Murray, D., Golebiewska, U., and McLaughlin, S. (2002) Lateral sequestration of phosphatidylinositol 4,5-bisphosphate by the basic effector domain of myristoylated alanine-rich C kinase substrate is due to nonspecific electrostatic interactions. *J. Biol. Chem. 277*, 34401–34412.
23. Hokanson, D. E., and Ostap, E. M. (2006) Myo1c binds tightly and specifically to phosphatidylinositol 4,5-bisphosphate and inositol 1,4,5-trisphosphate. *Proc. Natl. Acad. Sci. U.S.A. 103*, 3118–3123.
24. Liu, A. P., and Fletcher, D. A. (2006) Actin polymerization serves as a membrane domain switch in model lipid bilayers. *Biophys. J. 91*, 4064–4070.
25. Gokhale, N. A., Abraham, A., Digman, M. A., Gratton, E., and Cho, W. (2005) Phosphoinositide specificity of and mechanism of lipid domain formation by annexin A2-p11 heterotetramer. *J. Biol. Chem. 280*, 42831–42840.
26. Wagner, M. L., and Tamm, L. K. (2001) Reconstituted syntaxin1a/SNAP25 interacts with negatively charged lipids as measured by lateral diffusion in planar supported bilayers. *Biophys. J. 81*, 266–275.
27. Herrig, A., Janke, M., Austermann, J., Gerke, V., Janshoff, A., and Steinem, C. (2006) Cooperative adsorption of ezrin on PIP2-containing membranes. *Biochemistry 45*, 13025–13034.
28. Higgs, H. N., and Pollard, T. D. (2000) Activation by Cdc42 and $PIP_2$ of Wiskott-Aldrich syndrome protein (WASp) stimulates actin nucleation by Arp2/3 complex. *J. Cell Biol. 150*, 1311–1320.
29. An, X., Zhang, X., Debnath, G., Baines, A. J., and Mohandas, N. (2006) Phosphatidylinositol-4,5-biphosphate ($PIP_2$) differentially regulates the interaction of human erythrocyte protein 4.1 (4.1R) with membrane proteins. *Biochemistry 45*, 5725–5732.
30. Moens, P. D., and Bagatolli, L. A. (2007) Profilin binding to submicellar concentrations of phosphatidylinositol (4,5) bisphosphate and phosphatidylinositol (3,4,5) trisphosphate. *Biochim. Biophys. Acta 1768*, 439–449.
31. Roy, C., Martin, M., and Mangeat, P. (1997) A dual involvement of the amino-terminal domain of ezrin in F- and G-actin binding. *J. Biol. Chem. 272*, 20088–20095.
32. Andreoli, C., Martin, M., Le Borgne, R., Reggio, H., and Mangeat, P. (1994) Ezrin has properties to self-associate at the plasma membrane. *J. Cell Sci. 107* (Part 9), 2509–2521.
33. Huang, F. L., and Huang, K. P. (1991) Interaction of protein kinase C isozymes with phosphatidylinositol 4,5-bisphosphate. *J. Biol. Chem. 266*, 8727–8733.
34. Blin, G., Margeat, E., Carvalho, K., Royer, C. A., Roy, C., and Picart, C. (2008) Quantitative analysis of the binding of ezrin to large unilamellar vesicles containing phosphatidylinositol 4,5 bisphosphate. *Biophys. J. 94*, 1021–1033.
35. Pain, R. H. (2005) Determining the fluorescence spectrum of a protein, Current Protocols in Protein Science, Chapter 7, Unit 7.7, Wiley, New York.
36. Gorbatyuk, V. Y., Nosworthy, N. J., Robson, S. A., Bains, N. P., Maciejewski, M. W., Dos Remedios, C. G., and King, G. F. (2006) Mapping the phosphoinositide-binding site on chick cofilin explains how PIP2 regulates the cofilin-actin interaction. *Mol. Cell 24*, 511–522.
37. Liepina, I., Czaplewski, C., Janmey, P., and Liwo, A. (2003) Molecular dynamics study of a gelsolin-derived peptide binding to a lipid bilayer containing phosphatidylinositol 4,5-bisphosphate. *Biopolymers 71*, 49–70.
38. Smith, W. J., Nassar, N., Bretscher, A., Cerione, R. A., and Karplus, P. A. (2003) Structure of the active N-terminal domain of Ezrin. Conformational and mobility changes identify keystone interactions. *J. Biol. Chem. 278*, 4949–4956.
39. Li, Q., Nance, M. R., Kulikauskas, R., Nyberg, K., Fehon, R., Karplus, P. A., Bretscher, A., and Tesmer, J. J. (2007) Self-masking in an intact ERM-merlin protein: An active role for the central α-helical domain. *J. Mol. Biol. 365*, 1446–1459.
40. Nakamura, F., Huang, L., Pestonjamasp, K., Luna, E. J., and Furthmayr, H. (1999) Regulation of F-actin binding to platelet moesin in vitro by both phosphorylation of threonine 558 and polyphosphatidylinositides. *Mol. Biol. Cell 10*, 2669–2685.
41. Saarikangas, J., Zhao, H., and Lappalainen, P. (2010) Regulation of the actin cytoskeleton-plasma membrane interplay by phosphoinositides. *Physiol. Rev. 90*, 259–289.
42. Charras, G. T., Hu, C. K., Coughlin, M., and Mitchison, T. J. (2006) Reassembly of contractile actin cortex in cell blebs. *J. Cell Biol. 175*, 477–490.
43. Carvalho, K., Ramos, L., Roy, C., and Picart, C. (2008) Giant unilamellar vesicles containing phosphatidylinositol(4,5)bisphosphate: Characterization and functionality. *Biophys. J. 95*, 4348–4360.